Effect of Sodium Doping in β-Tricalcium Phosphate on Its Structure and Properties

Laetitia Obadia,[†] Philippe Deniard,[‡] Bruno Alonso,[§] Thierry Rouillon,[†] Stéphane Jobic,[‡] Jérôme Guicheux,[†] Marion Julien,[†] Dominique Massiot,[§] Bruno Bujoli,*[,||] and Jean-Michel Bouler[†]

INSERM, UMRS 791, Laboratoire d'Ingénierie Ostéo-articulaire et Dentaire (LIOAD), Faculté de chirurgie dentaire, Université de Nantes, BP 84215, 44042 Nantes Cedex 1, France, Institut des Matériaux Jean Rouxel, Université de Nantes, CNRS, UMR 6502, 2 Rue de la Houssinière, BP 92208, 44322 Nantes Cedex 3, France, CRMHT, UPR CNRS 4212, 1D Avenue de la Recherche Scientifique, 45071 Orléans Cedex 02, France, and Laboratoire de Synthèse Organique, Université de Nantes, CNRS, UMR 6513, Faculté des Sciences et des Techniques, 2 rue de la Houssinière, BP 92208, 44322 Nantes Cedex 3, France

Received September 22, 2005. Revised Manuscript Received January 9, 2006

For the preparation of β-TCP and biphasic calcium phosphates (BCPs, mixtures of hydroxyapatite and β-TCP), the presence of sodium in the reaction medium results in the incorporation of sodium in the β-TCP network, by substitution of some calcium sites. Accordingly, a decrease of the unit cell volume of β-TCP was observed with increasing sodium substitution. The distribution of sodium in the β-TCP structure, as a function of the amount incorporated, was probed using ^{31}P and ^{23}Na MAS NMR and $^{31}P\{^{23}Na\}$ REDOR experiments. It was shown that an estimation of the sodium content in β-TCPs could be obtained from the modeling of their ^{31}P MAS NMR spectra. Moreover, the incorporation of sodium in β-TCPs results in improved mechanical properties, without affecting the biocompatibility of the ceramics.

Introduction

Biphasic calcium phosphate (BCPs) ceramics, combinations of β-TCP [tricalcium phosphate, β-$Ca_3(PO_4)_2$] and HA [hydroxyapatite, $Ca_{10}(PO_4)_6(OH)_2$], are commonly used as bioactive implants in human bone surgery.[1−7] Indeed, such biomaterials with suitable composition and porosity are slowly resorbed in the body, releasing phosphates and calcium ions that are used by the organism for regenerating natural bone. The method currently recommended by manufacturing standards to control the quality of BCPs (HA/β-TCP ratio, inorganic impurities) is powder X-ray diffraction in addition to infrared spectroscopy.[8−10]

However, some results obtained in a recent work suggested that this method is not sufficient to determine the purity of the components in BCP. Indeed, as part of a study aimed at designing implantable calcium phosphate-based bisphosphonate local delivery systems,[11,12] a series of BCPs obtained via different preparation routes were studied as potential carriers for Zoledronate, a highly potent antiresorptive drug active against osteoporosis[13] and bone metastases.[14−17] In this context, the presence of the bisphosphonate sorbed onto the BCPs was probed using ^{31}P solid-state NMR spectroscopy. Surprisingly, although similar powder XRD patterns were observed for the BCP starting materials, their ^{31}P NMR signals were significantly different according to their synthesis mode (Figure 1). The presence of one peak at the expected chemical shift (2.8 ppm) for the HA component in

* To whom correspondence should be addressed. E-mail: bujoli@chimie.univ-nantes.fr. Fax: +33 251125402.
† Laboratoire d'Ingenierie Osteo-articulaire et Dentairé, Université de Nantes.
‡ Institut des Matériaux Jean Rouxel, Université de Nantes.
§ CRMHT.
|| Laboratoire de Synthese Organique, Université de Nantes.

(1) Cavagna, R.; Daculsi, G.; Bouler, J. *J. Long-Term Eff. Med. Implants* **1999**, *9*, 403.
(2) Gouin, F.; Delecrin, J.; Passuti, N.; Touchais, S.; Poirier, P.; Bainvel, J. *Rev. Chir. Orthop. Repar. Appar. Mot.* **1995**, *81*, 59.
(3) Passuti, N.; Daculsi, G.; Rogez, J.; Martin, S.; Bainvel, J. *Clin. Orthop.* **1989**, *46*, 169.
(4) Passuti, N.; Daculsi, G. *Presse Med.* **1989**, *18*, 28.
(5) Ransford, A.; Morley, T.; Edgar, M.; Webb, P.; Passuti, N.; Chopin, D.; Morin, C.; Michel, F.; Garin, C.; Pries, D. *J. Bone Joint Surg. Br.* **1998**, *80*, 13.
(6) Vallet-Regi, M.; Gonzalez-Calbet, J. M. *Prog. Solid State Chem.* **2004**, *32*, 1.
(7) Dorozhkin, S.; Epple, M. *Angew. Chem., Int. Ed.* **2002**, *41*, 3130.
(8) Ishikawa, K.; Ducheyne, P.; Radin, S. *J. Mater. Sci. Mater. Med.* **1993**, *4*, 165.
(9) Toth, J.; Hirthe, W.; Hubbard, W.; Brantley, W.; Lynch, K. *J. Appl. Biomater.* **1991**, *2*, 37.
(10) *Standard Specification for Composition of Ceramic Hydroxyapatite for Surgical Implants*; ASTM Standard F 1185-88; ASTM International: West Conshohocken, PA, 1993.
(11) Josse, S.; Faucheux, C.; Soueidan, A.; Grimandi, G.; Massiot, D.; Alonso, B.; Janvier, P.; Laïb, S.; Gauthier, O.; Daculsi, G.; Guicheux, J.; Bujoli, B.; Bouler, J. M. *Adv. Mater.* **2004**, *16*, 1423.
(12) Josse, S.; Faucheux, C.; Soueidan, A.; Grimandi, G.; Massiot, D.; Alonso, B.; Janvier, P.; Laib, S.; Pilet, P.; Gauthier, O. *Biomaterials* **2005**, *26*, 2073.
(13) Wilder, L.; Jaeggi, K.; Glatt, M.; Müller, K.; Bachmann, R.; Bisping, M.; Born, A.; Cortesi, R.; Guiglia, G.; Jeker, H.; Klein, R.; Ramseier, U.; Schmid, J.; Schreiber, G.; Seltenmeyer, Y.; Green, J. *J. Med. Chem.* **2002**, *45*, 3721.
(14) Rosen, L. S.; Gordon, D.; Kaminski, M.; Howell, A.; Belch, A.; Mackey, J.; Apffelstaedt, J.; Hussein, M.; Coleman, R. E.; Reitsma, D. J.; Seaman, J. J.; Chen, B.-L.; Ambros, Y. *Cancer J.* **2001**, *7*, 377.
(15) Saad, F.; Gleason, D. M.; Murray, R.; Tchekmedyian, S.; Venner, P.; Lacombe, L.; Chin, J. L.; Vinholes, J. J.; Goas, J. A.; Chen, B.-L. *J. Natl. Cancer Inst.* **2002**, *94*, 1458.
(16) Rosen, L. S.; Gordon, D.; Tchekmedyian, S.; Yanagihara, R.; Hirsh, V.; Krzakowski, M.; Pawlicki, M.; De Souza, P.; Zheng, M.; Urbanowitz, G.; Reitsma, D. J.; Seaman, J. J. *J. Clin. Oncol.* **2003**, *21*, 3150.
(17) Perry, C. M.; Figgitt, D. P. *Drugs* **2004**, *64*, 1197.

10.1021/cm052135f CCC: $33.50 © 2006 American Chemical Society
Published on Web 02/11/2006

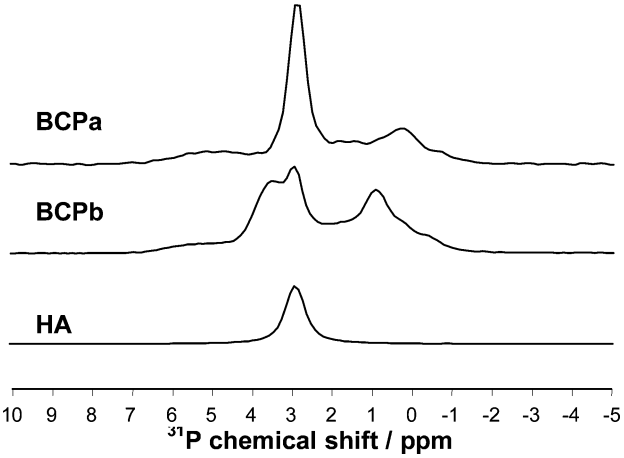

Figure 1. ^{31}P single-pulse MAS NMR spectra of BCP (HA50−TCP50) compounds obtained by two different preparation routes. The spectrum of a pure HA sample is given for comparison [$\nu_0(^{31}P)$ is 121.5 MHz for BCPa and 162.0 MHz for BCPb and HA).

all NMR spectra suggested that the observed difference might arise from some variation in the composition of the β-TCP component.

To confirm this hypothesis, a series of β-TCP phases were prepared in the present study according to different methods, including direct solid-phase synthesis along with calcination of precursors obtained by soft chemistry routes. In this article, we demonstrate, on the basis of ^{31}P and ^{23}Na solid-state NMR analyses of the resulting β-TCP compounds, that some calcium sites can be partly replaced by sodium when present in the reaction medium, leading to a modification of the environment of the different phosphorus sites. This results in an evolution of the ^{31}P NMR spectra, the simulation of which was found to be a convenient method for determining the sodium content. Moreover, the presence of sodium in β-TCPs led to increased compressive strengths, without affecting their biocompatibility.

Experimental Section

Materials and Methods. *X*-ray powder diffraction (XRD) patterns of BCPs and β-$Ca_{10.5-x/2}Na_x(PO_4)_7$ powders were recorded using a Philips PW 1830 generator equipped with a vertical PW 1050 ($\theta/2\theta$) goniometer and a PW 1711 Xe detector. The data were acquired using Ni-filtered copper Kα radiation in a step-by-step mode with 2θ initial = 10°, 2θ final = 100°, step 2θ = 0.03°, time per step = 2.3 s. Rietveld refinements were carried out to determine the unit cell parameters and atomic positions using WinPlotr[18] and Fullproff[19] as the graphical user interface and Rietveld refinement software, respectively. All diffraction patterns were refined using the Caglioti function for the diffraction profile. TiO_2 anatase powder (Merck) (around 10% w/w) was mixed with the samples to determine the amorphous phase percentage.[20] Energy-dispersive X-ray spectroscopy (EDXS) measurements were carried out on a LEO 1450 VP (Zeiss, Germany) scanning electron microscope (SEM) with an Oxford Inca X-slight 7353 attachment. The determination of the sodium content in the β-TCP phases was performed by atomic absorption spectrometry, using a Unicam 989 spectrometer equipped with a Na lamp. For the analyses, 100 mg of each sample was dissolved in 2 mL of a 10% HCl solution that was then diluted using a 0.2% KCl solution, and the analyses were performed at 589 nm with an air/acetylene flame. Fourier transform infrared (FTIR) spectra were obtained on a Nicolet Magnat II 550 FTIR spectrometer (400−4000 cm^{-1} spectral range with 4 cm^{-1} resolution and 128 scans), using the usual KBr pellet technique (1 mg of sample in 300 mg of KBr). Solid-state magic-angle-spinning nuclear magnetic resonance (MAS NMR) conditions were as follows: Longitudinal relaxation times T_1 for ^{31}P sites in β-TCP were measured and found to vary between 10 and 15 s [$\nu_0(^{31}P)$ = 121.5 MHz]. For Na-substituted β-TCP samples, longer relaxation times ($50 < T_1 < 300$ s) were found. In particular, the values were 90, 210, and 130 s for the main resonances located at 3.5, 2.3, and 0.8 ppm, respectively. ^{31}P single-pulse spectra were recorded in a single scan after a delay of 600 s. Single decaying exponential functions were used for apodization (line broadening below 10 Hz, representing 10% of the line width or less). The spectrometers used were Bruker 300, 400, and 750 models [$\nu_0(^{31}P)$ = 121.5, 162.0, and 303.7 MHz, respectively].

^{23}Na single-pulse NMR spectra were recorded on a Bruker 750 spectrometer [$\nu_0(^{23}Na)$ = 198.4 MHz] using a 14-kHz MAS rate (4-mm rotor), RF field strengths of 25 kHz, single $\pi/12$ RF pulses, recycle delays of 5 s, and acquisition of four scans. ^{23}Na triple-quantum 2D experiments were run on a Bruker 400 spectrometer [$\nu_0(^{23}Na)$ = 105.8 MHz], using an MQ z-filter pulse sequence,[21] a 13-kHz MAS rate (4-mm rotor), an RF field strength of 25 kHz, and recycle delays of 1 s with presaturation; 240 scans were recorded, with 256 slices in the F1 indirect dimension.

^{31}P{^{23}Na} REDOR experiments[22] were performed on a Bruker 400 spectrometer [$\nu_0(^{31}P)$ = 162.0 MHz, $\nu_0(^{23}Na)$ = 105.8 MHz], using a 25-kHz MAS rate (2.5-mm rotor), RF field strengths of 50 kHz for ^{31}P and 25 kHz for ^{23}Na (selective π pulses of 10 μs), recycle delays of 30 s with presaturation for ^{31}P, and acquisition of 32 scans at 32 different echo delays. Additional ^{23}Na{^{31}P} REDOR experiments were run on Bruker 400 or 750 spectrometers using the same range of RF fields.

^{31}P and ^{23}Na chemical shifts were referenced to external aqueous H_3PO_4 (85%) and aqueous NaCl (1 M), respectively. NMR spectra were modeled using the home-developed and freely available dmfit software.[23] Modeling of the ^{23}Na quadrupolar line shape was realized using the amorphous model line shape of the dmfit software. From this, we

(18) Roisnel, T.; Rodriguez-Carvajal, J. *Mater. Sci. Forum* **2001**, *378−381*, 118.
(19) Rodriguez-Carvajal, J.; Roisnel, T. In *Newsletter No. 20: Extended Software/Methods Development Issue*; Commission for Powder Diffraction, International Union of Crystallography: Stuttgart, Germany, 1998; pp 35−36.
(20) Orlhac, X.; Fillet, C.; Deniard, P.; Dulac, A.; Brec, R. *J. Appl. Crystallogr.* **2000**, *34*, 114.
(21) Amoureux, J.-P.; Fernandez, C.; Steuernagel, S. *J. Magn. Reson. A* **1996**, *123*, 116.
(22) Pan, Y.; Guillon, T.; Schaefer, J. *J. Magn. Reson.* **1990**, *90*, 330.
(23) Massiot, D.; Fayon, F.; Capron, M.; King, I.; Le Calve, S.; Alonso, B.; Durand, J. O.; Bujoli, B.; Gan, Z.; Hoatson, G. *Magn. Reson. Chem.* **2002**, *40*, 70.

extracted the ΔC_Q parameter that corresponds to the full width at half-maximum of the C_Q distribution.

Synthesis. TCPSolid was obtained by solid-phase reaction from a mixture of $CaHPO_4$ (9.108 g) and $CaCO_3$ (3.336 g) that was ground for 30 min and sintered at 1000 °C for 24 h. TCPNaOH was synthesized by hydrolysis of dicalcium phosphate dihydrate powder (DCPD, 90 g, Merck, Darmstadt, Germany) in 500 mL of a 0.6 mol L^{-1} NaOH solution. This reaction was performed under gentle stirring for 4 h at 90 °C, and the resulting solid was filtered, rinsed with water, dried in air, and calcined at 1000 °C for 4 h. $TCPNH_4OH$ was obtained by hydrolysis of DCPD (40 g) in 500 mL of a 0.3 mol L^{-1} NH_4OH solution. The reaction was performed under gentle stirring for 4 h at 90 °C, and the resulting solid was filtered, rinsed with water, dried in air, and calcined at 1000 °C for 4 h. TCPPrecip was prepared by precipitation of a 0.6 mol L^{-1} $Ca(OH)_2$ solution, obtained by the dropwise addition of 500 mL of a 0.4 mol L^{-1} H_3PO_4 solution. The solution was then stirred for 2 h, and the obtained gel was filtered, rinsed with water, dried in air, and calcined at 1000 °C for 4 h. Na-doped β-TCP samples of various compositions [$Ca_{10.5-x/2}Na_x(PO_4)_7$; $x = 0, 0.25, 0.5, 0.75, 1.0$) were prepared by solid-phase reaction using suitable stoichiometric proportions of $CaHPO_4$, $CaCO_3$, and Na_2CO_3. Reagents were mixed intimately, and then 20 cylindrical pellets (diameter, 20 mm; thickness, 5 mm) were prepared for each composition via uniaxial compression. Microporous ceramics were obtained after sintering the pellets at 1000 °C for 4 h according to the reaction

$$7CaHPO_4 + \left(3.5 - \frac{x}{2}\right)CaCO_3 + \frac{x}{2}Na_2CO_3 \rightarrow Ca_{10.5-x/2}Na_x(PO_4)_7 + 3.5CO_2 + 3.5H_2O \quad (1)$$

Results and Discussion

Identification of the Influence of the Na Content in β-TCPs on Their ^{31}P NMR Data. Two β-TCP ceramics were prepared according to methods commonly reported in the literature, denoted TCPSolid (sintering of a $CaHPO_4$/$CaCO_3$ mixture) and TCPPrecip [precipitation of a $Ca(OH)_2$ solution by addition of aqueous H_3PO_4, followed by calcination of the resulting gel]. Moreover, two additional samples were prepared by calcination of calcium-deficient apatites (CDAs) synthesized by hydrolysis of dicalcium phosphate dihydrate (DCPD), using an aqueous base such as sodium hydroxide (TCPNaOH) or ammonium hydroxide ($TCPNH_4OH$).

Powder X-ray diffraction analyses gave similar results for the four samples, that exhibited the specific diffraction pattern of β-TCP; the absence of any amorphous impurity was confirmed by Rietveld refinement of the XRD patterns of the various samples mixed with TiO_2. However, the ^{31}P solid-state NMR spectra differed notably for the four compounds, especially in the case of TCPNaOH, for which at least two additional lines of significant intensity were present at 0.85 and 3.5 ppm (Figure 2).

Similar NMR lines at the same positions were observed in some BCPs previously studied (Figure 1), thus confirming that this phenomenon is closely related to the β-TCP component, which can probably undergo a chemical modification that does not significantly affect the X-ray diffraction pattern. Subsequent characterization of the β-TCP samples by energy-dispersive X-ray spectroscopy (EDXS) revealed that the variation of the ^{31}P NMR spectra was directly correlated to the presence of sodium in the sample. At the same time, some variations in the νPO_4 infrared absorption pattern were similarly observed (Figure 3), suggesting slightly different environments around the phosphate groups for the four compounds.

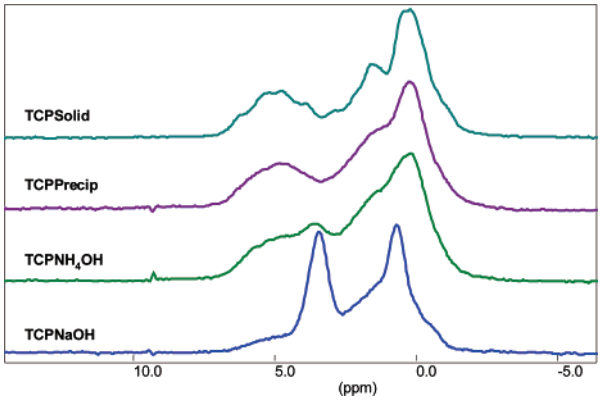

Figure 2. ^{31}P single-pulse MAS NMR spectra of the four β-TCPs obtained by different preparation routes (see text).

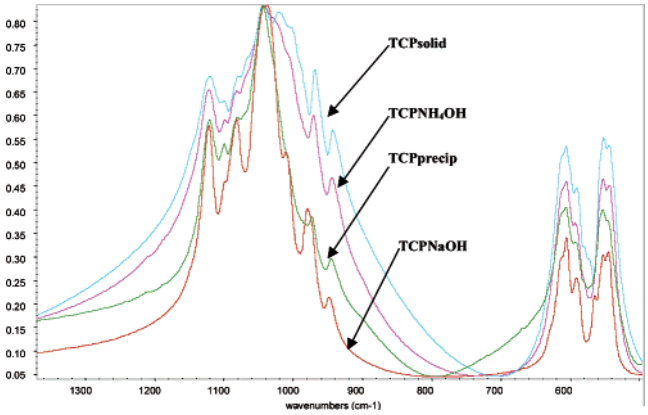

Figure 3. FTIR spectra of the four β-TCPs obtained by different preparation routes.

Table 1. Sodium Content Determined by AAS for DCPD and the β-TCP Samples

sample	Na content (wt %)
DCPD: $CaHPO_4 \cdot 2H_2O$	0.45 ± 0.01
TCPNaOH	1.44 ± 0.02
$TCPNH_4OH$	0.44 ± 0.01
TCPPrecip	0.000 ± 0.001
TCPSolid	0.000 ± 0.001

Whereas TCPPrecip and TCPSolid were shown to be sodium-free (Table 1) by atomic absorption spectroscopy (AAS), TCPNaOH and $TCPNH_4OH$ were found to contain 1.44 and 0.44 wt % sodium, respectively. Careful analysis of the synthesis protocol showed that the presence of sodium in the latter compound arose from the commercial DCPD starting material, which contained a similar amount of sodium (Table 1). Accordingly, a new batch of CDA was prepared from a sodium-free DCPD source and ammonium hydroxide, and after calcinations, the ^{31}P NMR spectrum of the corresponding TCP was similar to that recorded for TCP-

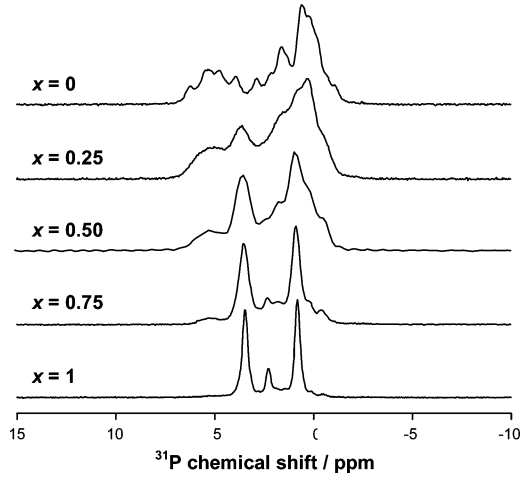

Figure 4. ^{31}P single-pulse MAS NMR spectra of $Ca_{10.5-x/2}$ $Na_x(PO_4)_7$ compounds, as a function of x [$\nu_0(^{31}P) = 303.7$ MHz].

Table 2. Na Content (wt %) in $Ca_{10.5-x/2}Na_x(PO_4)_7$ Compounds, Determined by AAS

x	theoretical	experimental
0	0	0.000 ± 0.001
0.25	0.53	0.54 ± 0.01
0.50	1.06	1.07 ± 0.02
0.75	1.59	1.61 ± 0.03
1	2.11	2.13 ± 0.03

Precip, with no sodium contamination. It was thus obvious that the presence of sodium in the reaction medium has an influence on the composition of the final TCP, via substitution of some of the calcium sites (ionic radius 1.00 Å) by sodium ions (ionic radius 0.99 Å). This was confirmed when a series of Na-doped tricalcium phosphates $Ca_{10.5-x/2}Na_x(PO_4)_7$ ($x = 0$, 0.25, 0.5, 0.75, 1) were prepared by direct high-temperature solid-phase synthesis, according to eq 1. Indeed, a strong variation of the ^{31}P NMR spectra of the corresponding solids (Figure 4) was observed as the Na content determined by atomic absorption spectroscopy increased (Table 2), leading to spectra very similar to those of $TCPNH_4OH$ ($x = 0.25$) and TCPNaOH ($x = 0.75$).

Effect of the Sodium Doping on the Local Environment of the Phosphorus Atoms in β-TCPs. The structure of pure β-TCP was determined by single-crystal X-ray diffraction by Dickens et al.[24] and later confirmed by Yashima et al.[25] through a neutron powder diffraction study. There are three crystallographically distinct phosphorus positions with 1:3:3 relative occupancies for P(1)/P(2)/P(3), as P(1) is on a crystallographically special position. The cations are distributed over five different sites, and of these, two cation sites [Ca(4) and Ca(5)] are special positions, one of which is half occupied [Ca(4)]. Among the three phosphorus sites, only P(1) and P(2) are each connected to a single Ca(4) site. As ^{31}P MAS NMR spectroscopy is very sensitive to local structural modifications, it is then expected that the corresponding resonances will differ according to whether the Ca(4) site is occupied or not, leading, in a first approximation, to five resonances in all: one for P(3), two equally intense lines for P(2), and the same for P(1). On this basis, Jakeman et al.[26] were able to simulate the β-TCP ^{31}P MAS NMR experimental spectrum satisfactorily, and the corresponding simulation performed with TCPPrecip is presented in Figure 5a: P(1) and P′(1) [7.1% and 4.2% (expected 7%)], P(2) and P′(2) [19.1% and 22.8% (expected 21.5%)], P(3) [46.8% (expected 43%)].

It is worth noting that (i) a deviation from the ideal ratio is observed, and some resonances are broader than others, as a probable result of positional disorder of the phosphorus atoms arising from the partial occupancy of the Ca(4) site, and (ii) a better ordering of the vacancies seems to be present for TCPSolid obtained by high-temperature direct synthesis, leading to a better-resolved ^{31}P MAS NMR spectrum, with at least 16 distinct resonances when the spectrum was recorded at very high magnetic field (Figure 5b). Actually, the assignment of these resonances is challenging and would require further 1D and 2D NMR experiments at different MAS rates and magnetic fields.

With substitution of sodium in the β-$Ca_3(PO_4)_2$ structure, a much simpler spectrum emerges as the sodium content increases (Figure 4). The ^{31}P spectrum of $Ca_{10.5-x/2}Na_x(PO_4)_7$ ($x = 1$) and its modeling are presented in Figure 6. The spectrum presents three main resonances (3.5, 2.3, and 0.8 ppm] with relative intensities in a ratio close to 4:1:4. It is important to note that, in addition to these main resonances, a series of weak peaks is also present in the spectrum. The latter probably denote the two insertion modes observed for sodium in $Ca_{10}Na(PO_4)_7$ (see next section) and can contribute to the deviation observed in the relative 3:1:3 intensity expected for the formation of $Ca_{10}Na(PO_4)_7$ in which the Ca(4) sites are fully occupied by sodium ions. Moreover, the intensity of the resonance at 2.3 ppm might be slightly underestimated because of its longer T_1 (see Experimental Section).

In addition to NMR measurements, XRD patterns were recorded as a function of the Na content in $Ca_{10.5-x/2}Na_x(PO_4)_7$. All of the corresponding structures were refined using the Rietveld method, starting from the previously mentioned structure proposed by Dickens et al.[24] No deviation from this latter structure was observed as a consequence of Na insertion, except for the unit cell parameters. This variation was found to differ depending on the β-TCP synthesis route: a nonmonotonic variation was obtained for all of the samples resulting from the calcination of precursors obtained by soft chemistry routes (i.e., TCPNaOH, $TCPNH_4OH$, and TCPPrecip), whereas direct solid-phase synthesis led to a quasi-perfect linear variation, especially for the c parameter, as reported in Figure 7. This monotonic variation in cell parameters was expected because of the different cation radius and oxidation state of sodium as compared to calcium.

To assign the new peaks observed in the ^{31}P NMR spectrum of $Ca_{10}Na(PO_4)_7$, we undertook a ^{31}P{^{23}Na} REDOR experiment,[22] which is sensitive to the dipolar couplings between ^{31}P and ^{23}Na nuclei and, thus, to their internuclear distances.[27] The experimental REDOR curves

(24) Dickens, B.; Schroeder, L. W.; Brown, W. E. *J. Solid State Chem.* **1974**, *10*, 232.
(25) Yashima, M.; Sakai, A.; Kamiyama, T.; Hoshikawa, A. *J. Solid State Chem.* **2003**, *175*, 272.
(26) Jakeman, R.; Cheetham, A.; Clayden, N.; Dobson, C. *J. Solid State Chem.* **1989**, *78*, 23.
(27) Guillon, T.; Schaefer, J. *J. Magn. Reson.* **1989**, *81*, 196.

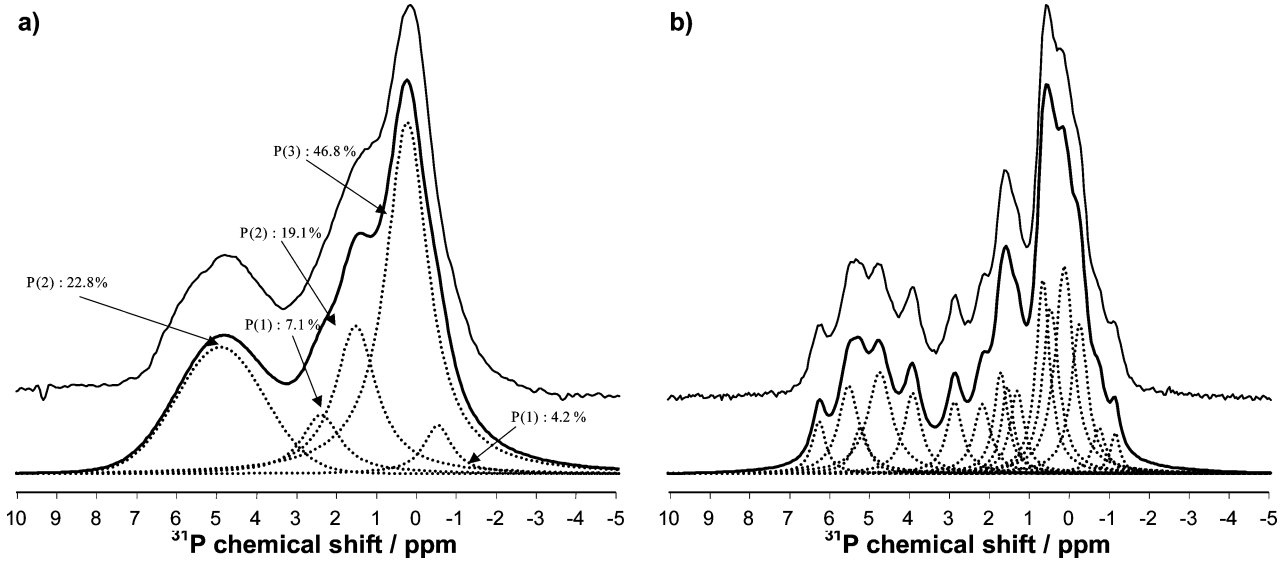

Figure 5. ^{31}P single-pulse MAS NMR spectra of β-TCP compounds and their modeling: (a) TCPPrecip [$\nu_0(^{31}P) = 162.0$ MHz], (b) TCPSolid [$\nu_0(^{31}P) = 303.7$ MHz].

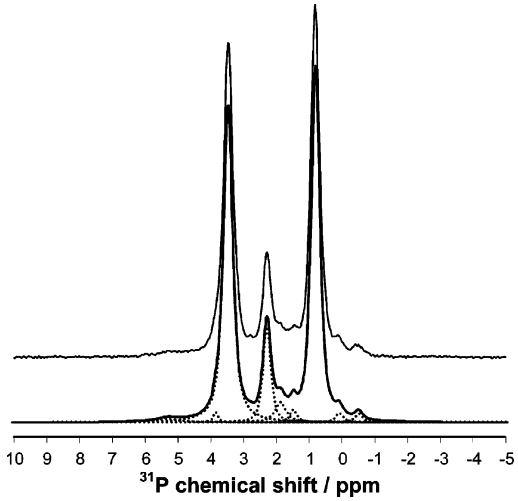

δ (ppm)	%	Assignment
5.30	1.3	
3.84	0.7	
3.46	40.2	P2-Na
2.78	0.1	
2.28	9.7	P1-Na
1.87	3.3	
1.48	1.3	
0.81	41.2	P3-Na
0.09	1.1	
-0.49	1.0	

Figure 6. ^{31}P single-pulse MAS NMR spectrum of $Ca_{10.5-x/2}Na_x(PO_4)_7$ ($x = 1$) and its modeling. The table shows the ^{31}P chemical shifts and the relative percentages of the areas of the ^{31}P deconvoluted peaks. Assignments are made on the basis of the ^{31}P{^{23}Na} REDOR results (see text).

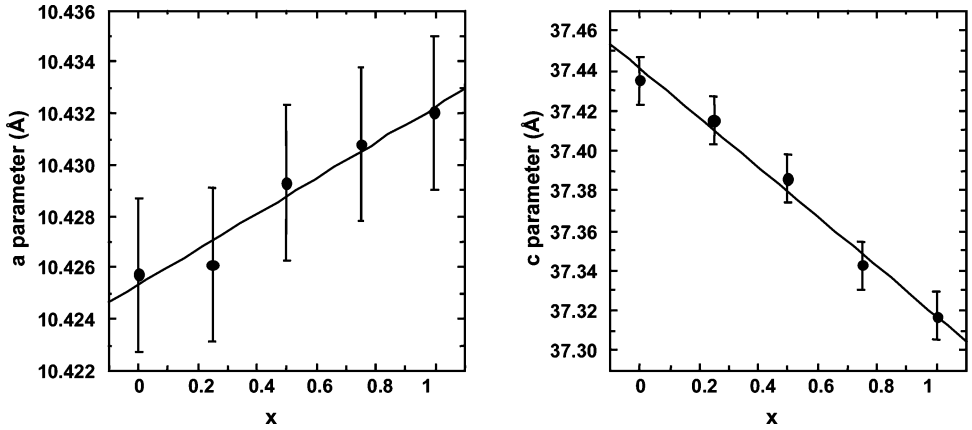

Figure 7. Variation of the cell parameters obtained from Rietveld structural refinement as a function of the Na content in $Ca_{10.5-x/2}Na_x(PO_4)_7$ compounds prepared by solid-phase reaction. The c values for TCPNaOH [$c = 37.292(5)$ Å] and TCPNH$_4$OH [$c = 37.389(4)$ Å] are given for comparison.

[i.e., the normalized signal difference $(S - S_0)/S_0$ as a function of the number of rotor periods N_{Tr}] are presented in Figure 8 for the three main peaks (located at 3.5, 2.3, and 0.8 ppm).

Information on the spatial proximities between the P and Na sites can be obtained theoretically from the initial slope of these REDOR curves. We have used the formula proposed by Bertmer and Eckert[28] for the initial variation of $(S - S_0)/S_0$ in the case of a pair of coupled spins and considering a

(28) Bertmer, M.; Eckert, H. *Solid State Nucl. Magn. Reson.* **1999**, *15*, 139.

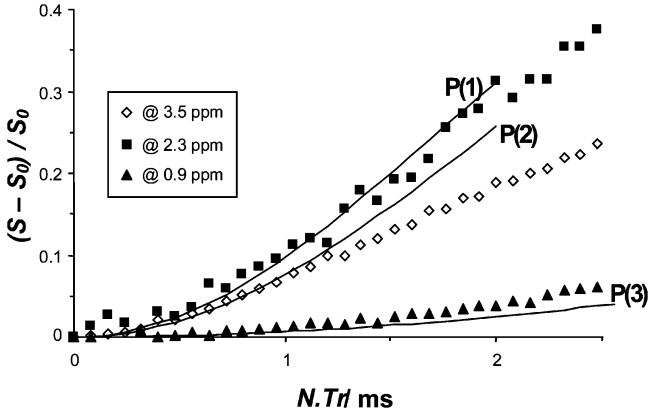

Figure 8. Experimental $^{31}P\{^{23}Na\}$ REDOR curves of $Ca_{10.5-x/2}Na_x(PO_4)_7$ ($x = 1$) obtained for the ^{31}P peaks located at 3.5, 2.3, and 0.8 ppm (open diamonds, solid squares, and solid triangles, respectively). Calculated curves for the three phosphorus sites of β-TCP (lines) take into account a complete insertion of Na into Ca(4) sites and a prefactor of $f = 0.6$ (see text for details).

second-order approximation for the REDOR signal. This approach is sufficient for the purposes of this study, although a more complete interpretation could be considered using model compounds and the procedure recently suggested for multispin systems that takes into account the effect of the quadrupolar interactions.[29] As we used near-selective ^{23}Na pulses in our experiment ($\nu_{RF}/\nu_Q \approx 0.02$), we have to take into account the fact that only the central transition $|+^1/_2\rangle \leftrightarrow |-^1/_2\rangle$ would be uniformly excited and the other transitions could be partially excited in these REDOR experiments.[30] Therefore, we introduced a multiplicative prefactor f as previously suggested,[31] leading to the formula:

$$\Delta S/S_0 = f.[16/15(N_{Tr})^2D^2 - 128/315(N_{Tr})^4D^4] \quad (2)$$

where D is the dipolar coupling for a given $^{31}P \approx ^{23}Na$ pair. D values were calculated using the P(1)−Ca(4), P(2)−Ca(4), and P(3)−Ca(4) internuclear distances (3.177, 3.320, and 5.064 Å, respectively) obtained from the published crystal structure of β-TCP.[24,25] The three curves for the P(1), P(2), and P(3) phosphorus sites are drawn in Figure 8 using $f = 0.6$. Considering only the excitation of the ^{23}Na central transition would lead to $f = 0.4$. The difference accounts for the non-purely selective pulses used, but also for possible adiabatic passages between $|\pm^1/_2\rangle$ and $|\pm^3/_2\rangle$ states—as in TRAPDOR[32,33] and REAPDOR[34] experiments—due to the experimental conditions [in particular, $\nu_{MAS} = 25$ kHz and ν_{RF} (^{23}Na) = 25 kHz]. Nevertheless, there is a relatively good agreement between the sets of experimental and calculated initial slopes of the REDOR curves. If we also consider the differences in intensity observed for the three main resonances (Figure 6), we can assign the peaks located at 3.5, 2.3, and 0.8 ppm to the P(2), P(1), and P(3) phosphorus sites, respectively, in a structure where Na occupies all of the Ca(4) sites of pure β-TCP.

(29) Strojek, W.; Kalwei, M.; Eckert, H. *J. Phys. Chem. B* **2004**, *108*, 7061.
(30) Chopin, L.; Vega, S.; Gullion, T. *J. Am. Chem. Soc.* **1998**, *120*, 4406.
(31) Chan, J. C. C.; Bertmer, M.; Eckert, H. *J. Am. Chem. Soc.* **1999**, *121*, 5238.
(32) van Eck, E. R. H.; Janssen, R.; Maas, W. E. J. R.; Veeman, W. S. *Chem. Phys. Lett.* **1990**, *174*, 428.
(33) Grey, C. P.; Veerman, W. S. *Chem. Phys. Lett.* **1992**, *192*, 379.
(34) Guillon, T. *Chem. Phys. Lett.* **1995**, *246*, 325.

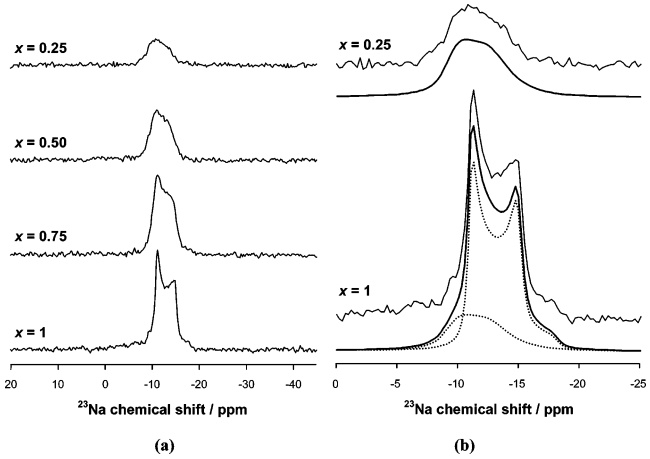

Figure 9. (a) ^{23}Na single-pulse MAS NMR spectra of $Ca_{10.5-x/2}Na_x(PO_4)_7$ compounds as a function of x [$\nu_0(^{23}Na) = 198.4$ MHz]. (b) Modeling of the ^{23}Na NMR spectra of $Ca_{10.5-x/2}$ $Na_x(PO_4)_7$ compounds ($x = 0.25$, $x = 1$).

Table 3. NMR Parameters of the Two ^{23}Na Signals Obtained by Modeling the ^{23}Na Spectra of $Ca_{10.5-x/2}Na_x(PO_4)_7$.($x = 0.25$ and 1)[a]

signal	δ_{iso} (ppm)	C_Q (MHz)	ΔC_Q (kHz)	η_Q
1	−8.3	2.2	380	∼0.3
2	−9.7	2.3	90−360	0.0

[a] See Experimental Section for details.

Local Environment of the Sodium Atoms as a Function of the Na Content in β-TCPs. The presence of sodium in the lattice was also evidenced by ^{23}Na MAS NMR spectroscopy. Single-pulse ^{23}Na spectra of $Ca_{10.5-x/2}Na_x(PO_4)_7$ compounds, as a function of x are presented in Figure 9a, showing a gradual evolution with increasing x. For the lowest value ($x = 0.25$), the signal is broad, suggesting a high level of disorder for the sodium sites. This was modeled by a second-order quadrupolar line shape (Figure 9b) with a high value of dispersion for the quadrupole coupling constant (ΔC_Q parameter for signal 1 in Table 3). For the highest value ($x = 1$), the spectrum presents a more defined and characteristic second-order quadrupolar line shape. However, this spectrum cannot be modeled accurately by a single contribution (signal 2, with $\Delta C_Q = 90$ kHz; see Table 3). A second and broader contribution, corresponding to signal 1, had to be used for a better simulation (Figure 9b).

To further investigate the existence of various ^{23}Na signals, we recorded a ^{23}Na triple-quantum 2D spectrum for $x = 1$ (Figure 10), showing that its projection onto the isotropic dimension is not symmetrical and can be deconvoluted into two Gaussian−Lorentzian functions. In addition, the whole triple-quantum 2D spectrum is better modeled using two contributions rather than one (not shown). Therefore, different kinds of sodium sites are present that can be associated with the two different signals 1 and 2. From $^{23}Na\{^{31}P\}$ REDOR experiments performed on various samples ($x = 0.5$, 0.75, 1), we observed that the two signals have similar REDOR curves and that both correspond to sodium atoms close to phosphorus sites. The differences between the two ^{23}Na signals deduced from modeling (Table 3) are the chemical shifts, the ΔC_Q quadrupolar coupling constant dispersion, and the η_Q asymmetry parameter. This might reflect slight differences in the geometry of the Ca(4) sites occupied by Na.

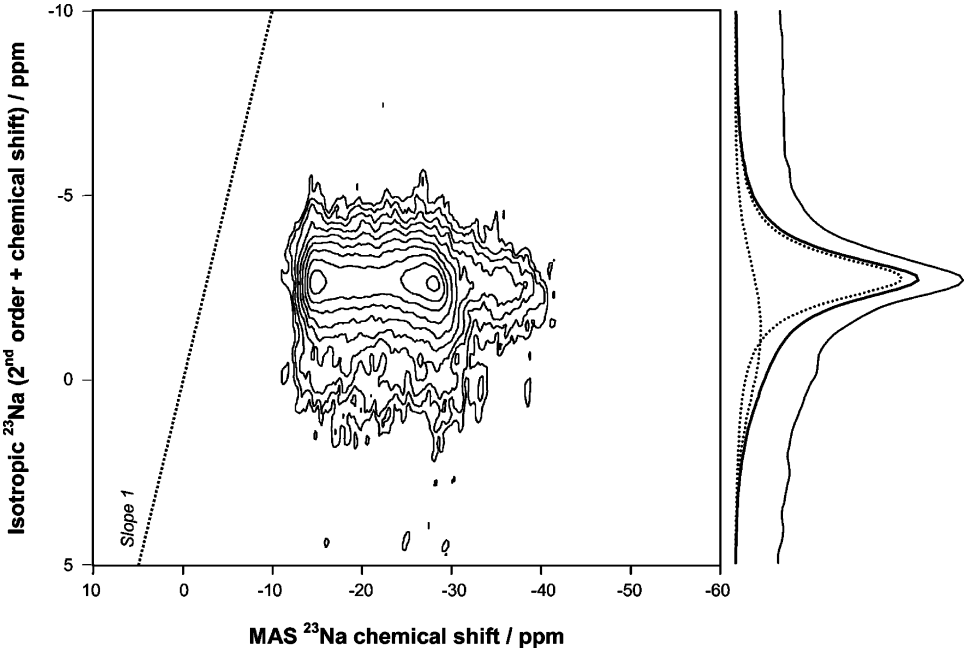

Figure 10. Sheared ^{23}Na triple-quantum MQMAS 2D obtained with an MQ *z*-filter pulse sequence [$\nu_0(^{23}\text{Na}) = 105.8$ MHz]. The projection onto the ^{23}Na vertical dimension and its deconvolution into two contributions are shown on the right side of the figure.

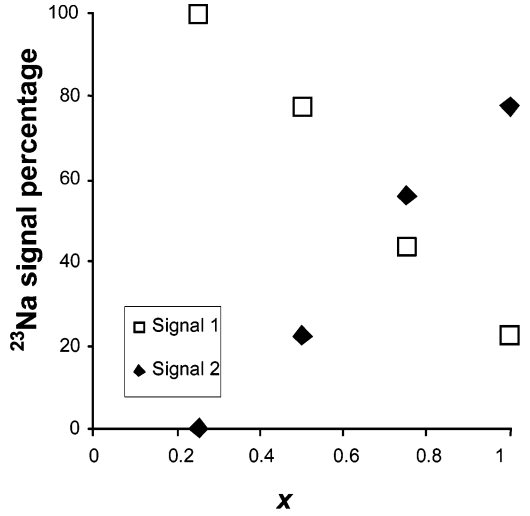

Figure 11. Variation of the relative percentages of the two ^{23}Na signals for $Ca_{10.5-x/2}Na_x(PO_4)_7$ compounds as a function of *x*.

Indeed, we tried to model the four ^{23}Na 1D spectra of Figure 9 using the two contributions with the set of parameters listed in Table 3. It was clearly necessary to vary the ΔC_Q parameter for signal 2 in order to obtain good simulations. In the case of $x = 0.5$, ΔC_Q reached 360 kHz, close to the value of signal 1. Accordingly, a gradual ordering of the sodium nuclei associated with signal 2 was observed as the sodium content increased. Moreover, the relative percentages between the two signals varied in an opposite way as a function of *x* (Figure 11). Signal 1 was the only signal observed at low values of *x*, whereas the narrow signal was detected from $x = 0.5$ and became majority only at $x = 0.75$. Even if the modeling of the spectra by two contributions could be formal, these variations clearly show that the insertion of Na into the Ca(4) sites leads to a $Ca_{10.5-x/2}Na_x(PO_4)_7$ disordered phase at the beginning, and not to a phase separation between $Ca_{10.5}(PO_4)_7$ and $Ca_{10}Na(PO_4)_7$ defined phases. This result is in full agreement with the variation of the unit cell parameters as a function of Na content observed from XRD measurements, as a biphasic composition should lead to two sets of cell parameters.

Evaluation of the Sodium Content. Although the sodium insertion in β-TCP appeared rather complicated, we were interested in determining whether an estimation of the Na content in β-TCPs could be obtained from simple and fast measurements.

A first possibility was investigated through the modeling of the ^{31}P MAS NMR spectra obtained at moderate magnetic fields [$\nu_0(^{31}\text{P}) = 121.5$ or 162.0 MHz]. In this context, we have shown that the ^{31}P MAS NMR spectra of the sodium-containing β-TCP could be simulated as the sum of two contributions: one corresponding to the five NMR signals of pure β-TCP (denoted A) and the other to the three NMR lines of $Ca_{10}Na(PO_4)_7$ (denoted B). As illustrated in Figure 12, a deconvolution of the spectra was performed on this basis, with fixed isotropic chemical shifts for the eight resonances (5 + 3) and refinement of the corresponding line widths and intensities. From the calculated spectra, the relative abundance of the two NMR patterns [area B/(area B + area A)] was found to be in good agreement with the experimental value of the sodium percentage *x* in $Ca_{10.5-x/2}Na_x(PO_4)_7$. This was also the case when similar modeling was applied to the ^{31}P MAS NMR spectra of TCPNaOH ($x = 0.63$ from the NMR simulation; $x = 0.68$ as determined by AAS) and $TCPNH_4OH$ ($x = 0.27$ from the NMR simulation; $x = 0.21$ as determined by AAS). Therefore, we can then conclude that, in a first approximation, the Na content in β-TCP phases can be conveniently determined by modeling the corresponding ^{31}P MAS NMR spectra, using a free-access laboratory-developed software available on the Internet.[23]

A second possible evaluation of the Na content in $Ca_{10.5-x/2}Na_x(PO_4)_7$ could be offered by XRD measurements through the variation of the *c* cell parameter as a function

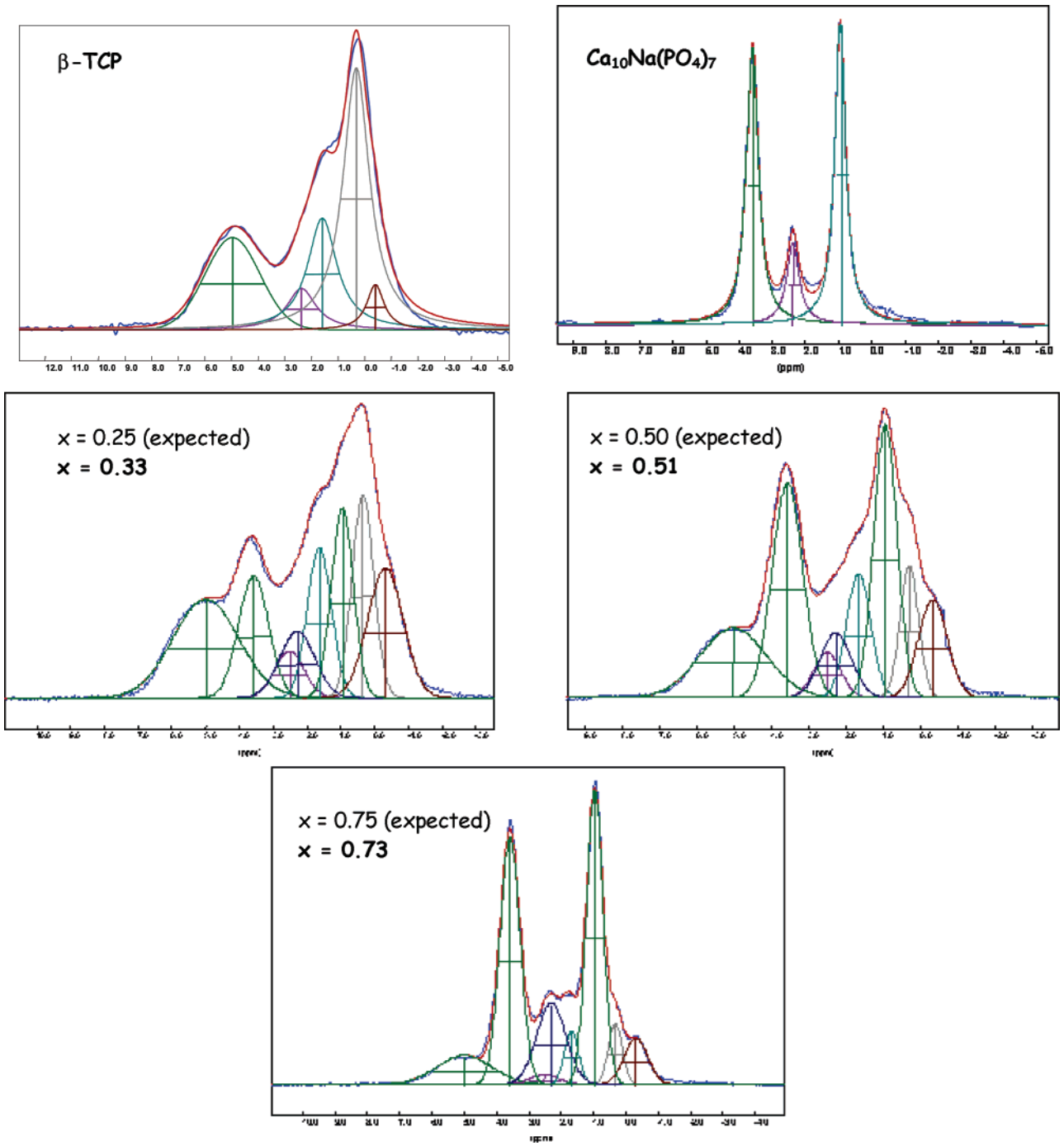

Figure 12. Simulation of the $Ca_{10.5-x/2}Na_x(PO_4)_7$ ^{31}P MAS NMR spectra as the sum of $Ca_{10.5}(PO_4)_7$ (pure β-TCP) and $Ca_{10}Na(PO_4)_7$ contributions. The relative abundance of the latter contribution (denoted x) is compared to the experimental value of the Na content [x (theory)].

of x (Figure 7). This could be very attractive given the recent development of new X-ray detectors that require approximately 2 min for the acquisition of a pattern having the same quality as those described in the Experimental Section of this article, instead of 2 h with classical scintillation detectors. In the present case, however, as mentioned above, this measurement is relevant only for samples prepared by solid-phase synthesis. Therefore, one can wonder why X-ray diffraction does not show a monotonic variation of the cell parameters as a function of the sodium content for samples prepared by calcination of precursors obtained by soft chemistry routes, whereas ^{31}P MAS NMR spectroscopy does not seem to be sensitive to this parameter. This could be related to a problem of structural origin that is not clearly mentioned in the literature: the crystallographic structure, as published on the basis of the single-crystal study reported by Dickens et al., shows an estimated valence[35,36] of 3 for the Ca(5) site. This result was confirmed by a recent neutron diffraction study,[25] in which the authors calculated this latter valence but did not comment on its abnormally high value. It is, of course, inconceivable to completely reject the β-TCP structure, but it would be interesting to refine it again from a single-crystal study, with the help of modern

(35) Brese, N. E.; O'Keeffe, M. *Acta Crystallogr.* **1991**, *B47*, 192.
(36) Brown, I. D. *Acta Crystallogr.* **1995**, *B48*, 553.

equipment. Indeed, powder diffraction is not the best method because of the large unit cell volume, which induces a strong overlap of the diffraction peaks that does not favor the measurement of their intensities with high precision. However, cell parameter refinements are independent of the intensity of the diffraction lines and are thus reliable, giving indirect information about the presence of a structural anomaly that still remains to be elucidated.

A full report on the mechanical properties and biocompatibility of Na-containing β-TCP will follow later, showing that a linear increase of the compressive strength was clearly observed for $Ca_{10.5-x/2}Na_x(PO_4)_7$ as the Na content was raised and that biocompatibility did not show any significant difference due to the presence of sodium (up to 2.11% by weight for $x = 1$) in the β-TCP structure.

Conclusion

We have shown that any source of sodium present during the synthesis of β-TCP resulted in sodium insertion in the ceramic network, the extent of which can easily be estimated using ^{31}P solid-state NMR spectroscopy. X-ray powder diffraction can also be used, but only for compounds obtained by solid-phase synthesis, provided that a careful Rietveld refinement is done to obtain very accurate unit cell parameters. At low sodium loading, highly disordered $Ca_{10.5-x/2}Na_x(PO_4)_7$ phases were formed, ending up in a well-ordered $Ca_{10}Na(PO_4)_7$ composition when the sodium amount x was increased, although some slight differences in the geometry of the Na sites were still present. This study also highlights a crystallographic issue that needs to be addressed through a careful single-crystal diffraction experiment.

Acknowledgment. This work was partially supported by the French Ministry of Research (ACI "Technologies pour la Santé") and the CNRS (Programme "Matériaux Nouveaux—Fonctionnalités Nouvelles"). Partial support from the Région Pays de la Loire (CER "Biomatériaux—S3") is also acknowledged.

CM052135F